



Pervaporation of the low ethanol content extracting stream generated from the dealcoholization of red wine by membrane osmotic distillation



Javier Esteras-Saz^{a,b}, Óscar de la Iglesia^{a,c}, Izumi Kumakiri^d, Cristina Peña^e, Ana Escudero^e, Carlos Téllez^{a,b}, Joaquín Coronas^{a,b,*}

^a Instituto de Nanociencia y Materiales de Aragón (INMA), CSIC-Universidad de Zaragoza, Zaragoza 50018, Spain

^b Chemical and Environmental Engineering Department, Universidad de Zaragoza, Zaragoza 50018, Spain

^c Centro Universitario de la Defensa Zaragoza, Academia General Militar, 50090 Zaragoza, Spain

^d Graduate School of Sciences and Technology for Innovation, Yamaguchi University, Ube 7558611, Japan

^e Laboratorio de Análisis del Aroma y Enología (LAAE), Department of Analytical Chemistry, Universidad de Zaragoza, Instituto Agroalimentario de Aragón (IA2) (UNIZAR-CITA), Associate Unit to Instituto de las Ciencias de la Vid y el Vino (ICVV) (UR-CSIC-GR), Zaragoza 50009, Spain

ARTICLE INFO

Article history:

Received 28 November 2022

Revised 31 January 2023

Accepted 15 February 2023

Available online 23 February 2023

Keywords:

Membrane

Polymer

Zeolite

Osmotic distillation

Dealcoholization

Pervaporation

ABSTRACT

This paper presents as main contribution the combination of membrane osmotic distillation (OD) to dealcoholize red wine with hydrophobic-hydrophilic pervaporation (PV) carried out to add value to the wastewater (extracting water) produced in OD, recycling water and generating bioethanol. Membrane OD with a commercial polypropylene hollow fiber module was applied to partially dealcoholize red wine from 14.0 to 11.0 v/v% ethanol. The OD extracting water, containing only ca. 5.3 wt% ethanol, was treated by sequential PV with both hydrophobic (PDMS or zeolite silicalite-1) and hydrophilic (zeolites mordenite or faujasite) membranes. This hydrophobic-hydrophilic PV produced two main products: bioethanol (recovering 88% of the ethanol removed from the wine) and a 99.4 wt% water-rich product. This water-rich product, with a very low ethanol content, was used as extracting water in the OD, giving rise to an analogous partially dealcoholized wine, in terms of aroma contents (as determined by gas chromatography for 25 compounds), to that achieved when using fresh water.

© 2023 The Author(s). Published by Elsevier B.V. on behalf of The Korean Society of Industrial and Engineering Chemistry. This is an open access article under the CC BY-NC-ND license (<http://creativecommons.org/licenses/by-nc-nd/4.0/>).

Introduction

Global warming, leading to obtain grapes with an excessive sugar concentration, is altering the cycle of wine. This results in wines with an undesirably high concentration of ethanol, which increases the solubility of some volatile compounds in wine and reduces its quality [1–3]. Different strategies have been developed to produce balanced wines with low alcoholic strength, those that remove the ethanol content from the finished wines being the most used [4–8].

In addition to the simple addition of water to grape must, usually restricted or only recently authorized in most of the wine producing countries [9], one of the most promising techniques to dealcoholize wine is based on membrane osmotic distillation (OD). This is a membrane operation able to work at low pressures and temperatures, hence diminishing the required energy costs

and the impact on the composition and sensory attributes of the processed wines. In fact, OD has already been used to dealcoholize, partial or totally, beer and wine [10–19]. In OD, the feed and the extracting solution (usually water) are faced by a hydrophobic membrane (typically of polypropylene, PP). As a result, the component concentration gradients between both membrane sides act as the driving force for the separation. The hydrophobic membrane prevents the entry of the aqueous solution into the pores, while the use of water as stripper creates an ethanol vapor pressure difference between both membrane sides which increases the ethanol flux and reduces the water activity across the membrane and therefore its transport [20]. The rest of minor components, with much lower concentrations than ethanol, should preferentially remain in the feed.

OD is considered as a clean technology [9], due to the fact that the extracting solution generated is essentially water with a low ethanol content and minimum amounts of aromas from wine. Up to date, this extracting solution is not reused and becomes a waste due to the fact that its ethanol concentration is very low, often around 5 wt% or even less [12,21,22]. Consequently, the used water

* Corresponding author at: Instituto de Nanociencia y Materiales de Aragón (INMA), CSIC-Universidad de Zaragoza, Zaragoza 50018, Spain.

E-mail address: coronas@unizar.es (J. Coronas).

in relation to the processed wine is high (with a minimum ratio of 0.5 liter of water per liter of wine [12]), representing an important economic loss and hampering the OD development and its implementation in wineries. Developing a separation stage for the extracting solution would allow the recycle of water, reducing the generation of wastewater close to zero and producing an alcohol-rich stream, which could in turn be regarded as second generation (2G) bioethanol (i.e. not produced from direct fermentation of sugars, see below for further details). All this would make the process of wine dealcoholization by OD more sustainable and favorable.

Bioethanol is the most popular biofuel since it can be mixed with petrol in different proportions or even used directly as fuel for transportation [23,24]. Furthermore, bioethanol can be produced by fermentation of cheap and abundant agricultural by-products rich in sugars or starch, like those related to rice, millet, sorghum or sugar-cane [25–29]. In fact, bioethanol production through this way, giving rise to first generation (1G) bioethanol, has been growing steadily since the 1920's [30,31]. Nevertheless, the use of food materials as feedstock has increased the cost-effectiveness of 1G bioethanol, restraining the growth of biofuels as an alternative to petrol [32]. Therefore, the current trend is the production of the so-called 2G bioethanol, which can be obtained from inexhaustible raw materials [33,34]. The search for cheap and abundant sources of raw material is an important issue to develop the production of 2G bioethanol [35,36] and OD waste could help meet its demand.

Moreover, the separation of ethanol as minor component by a typical distillation is ineffective. Thus, pervaporation (PV) appears as an interesting separation operation, which has already been used to dehydrate concentrated alcohol solutions and, to a minor extent, for the ethanol recovery from diluted hydroalcoholic solutions [37]. Under these conditions, PV constitutes a clear alternative to distillation [38,39]. In addition, PV is accepted as an energy-saving operation to separate close boiling point and azeotropic mixtures due to its high separation selectivity, reasonable flux, and low operational cost [40–45]. PV can be carried out either with hydrophilic or hydrophobic membranes. Hydrophilic membranes allow the dehydration of a given organic solvent or the separation of the most polar component of an organic mixture; on the contrary, hydrophobic ones provide the preferential permeation of the least polar component of a certain mixture [46,47].

When dealing with diluted alcohol solutions, an interesting approach is the sequential hydrophobic-hydrophilic PV. This process, recently validated through theoretical and economic studies [48,49], uses a hydrophobic membrane to remove alcohol from the diluted alcohol solutions to subsequently dehydrate the alcohol-rich permeate with a hydrophilic membrane. This is the case of the anhydrous ethanol production by a hydrophobic (PDMS)-hydrophilic (carboxymethyl cellulose) PV [50] and when applying (PDMS)-hydrophilic (polyvinyl alcohol) PV to diluted isobutanol aqueous solutions [51].

In this work, a red wine was partially dealcoholized by membrane OD using pure water as extracting agent, following our previously developed OD methodology based on the application of PP membranes [12]. Next, the wastewater obtained (a dilute hydroalcoholic solution) was treated by hydrophobic-hydrophilic PV. As shown in Fig. 1, hydrophobic PV (HFB-PV), using PDMS or zeolite silicalite-1 membranes, was directly applied to the OD waste. Subsequently, the permeate from the HFB-PV was dehydrated by hydrophilic pervaporation (HPL-PV), using faujasite or mordenite zeolite membranes. As a consequence, bioethanol and water were obtained. This water (with very low ethanol content) was reused as stripping agent in a new OD operation of wine dealcoholization. This wine was compared in terms of aroma composition with that obtained by typical OD, using pure water as extracting agent. To the best of our knowledge the hydrophobic-hydrophilic PV process

proposed here, has never been applied to process the wastewater from membrane OD treated wine, this being the main achievement of this work.

The demonstration of the feasibility of this OD-PV combination will help the up-scaling of the technology. In fact, a life cycle analysis (LCA) of wine dealcoholization by OD demonstrated its low environmental impact [52], while hydrophilic PV is commercially available for ethanol (and other solvents) dehydration since many years ago [53] and recently PV has been presented as a promising method for the bioethanol separation in an industrial context [39]. Last but not least, the sustainability of the OD-PV intensified process is of paramount importance, since, beyond the use of membranes as a low cost tool, the proposed solution agrees with the rule of the three Rs (reduce, reuse and recycle) within the framework established by the 2030 Sustainable Development Agenda.

Materials and methods

Membranes

The OD membrane module is equipped with Liqui-Cel™ MM-1x5.5 hydrophobic porous polypropylene (PP) hollow fiber membranes from 3M™. The main characteristics of the membrane module are: 2300 hollow fibers with inner and outer diameters of 220 and 300 μm , thickness of 40 μm and nominal pore size of 30 nm. The effective length is 14 cm yielding a 0.18 m^2 of membrane area.

Concerning PV, hydrophobic flat sheet membranes (15 cm^2 of membrane area) of PDMS were purchased to Deltamem AG (PDMS™ 4060), while tubular zeolite membranes (25 cm^2 of membrane area; 1.2 cm of outer diameter and 0.86 cm of inner diameter) of hydrophobic silicalite-1 (MFI type structure with pores of 0.51 \times 0.55 nm and 0.53 \times 0.56 nm) and hydrophilic mordenite (MOR type structure with pores of 0.26 \times 0.57 nm and 0.65 \times 0.7 nm) and faujasite (FAU type structure with pores of 0.74 nm) were prepared on mullite tubular supports following previous reports. Silicalite-1 membranes (SIL) with ca. 10 μm thickness were obtained by rubbing seeding followed by secondary growth [54]. In detail, silicalite-1 nanoseeds of 100 nm were obtained with a 1SiO₂: 0.36TPAOH: 20H₂O gel at 130 °C for 48 h, TPAOH being tetrapropylammonium hydroxide. These nanoseeds were applied mechanically to the outer surface of tubular supports. Then, silicalite-1 (SIL) membranes were prepared by secondary growth carried out with a 1SiO₂: 0.20TPAOH: 0.10TPABr: 0.10NH₄F: 500H₂O gel at 185 °C for 12 h, where TPABr is tetrapropylammonium bromide [54]. SIL membranes were calcined at 500 °C for 20 h to remove the organic structure directing agent (OSDA) used for their synthesis. Mordenite (MOR) and faujasite (FAU) membranes with ca. 1 μm thickness were prepared by crystallization but without OSDA, therefore they were not calcined [55,56]. In detail, MOR membranes were crystallized at 170 °C for 6 h with a 1SiO₂: 0.08Al₂O₃: 0.2Na₂O: 0.1NaF: 35H₂O gel previous rubbing seeding with MOR commercial crystals (Wako) [55], while FAU membranes were also obtained after rubbing seeding with Si/Al = 2.5 NaY commercial crystals (Wako) and secondary hydrothermal synthesis at 80 °C for 6 h with a 25SiO₂: 1Al₂O₃: 72Na₂O: 990H₂O gel [56].

The physicochemical characterization of the zeolite membranes was not addressed in this work since this has been previously reported in the just given citations [54–56].

Osmotic distillation experimental setup

Fig. 1 shows the schematic representation of the laboratory approach for coupling OD and PV membrane processes. A complete

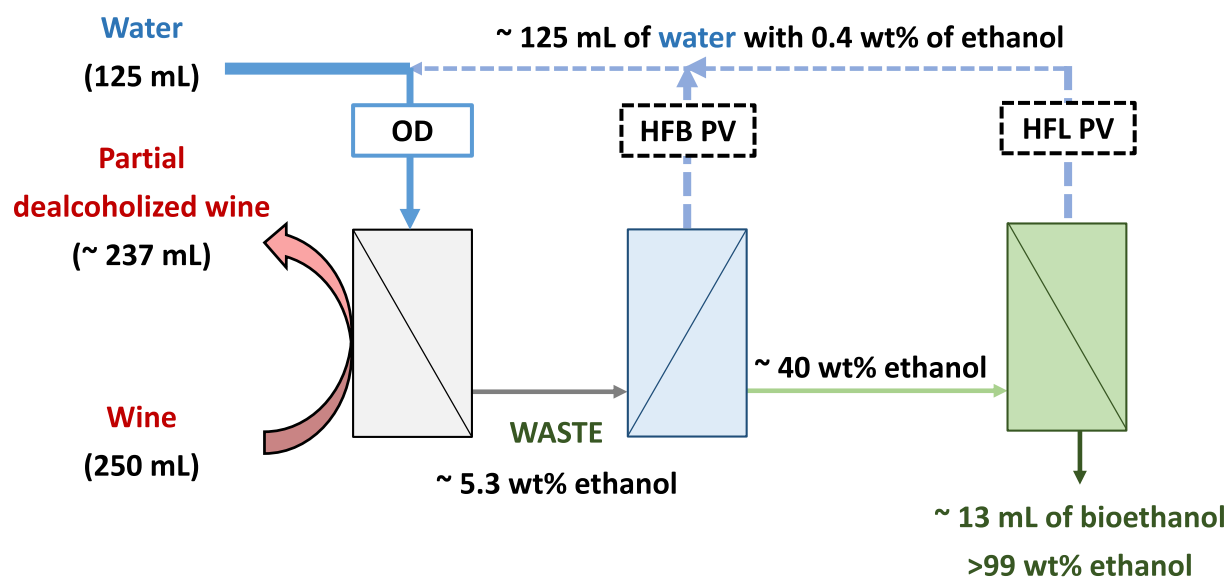


Fig. 1. General scheme of the osmotic distillation-pervaporation coupling.

description of the membrane OD lab-scale plant can be found elsewhere [12]. Briefly, this includes the membrane module with feed (Q_f) and extracting (Q_e) flow systems, pressure and temperature controllers. A chiller bath Julabo™ (Corio-201F) maintains the desired temperature on both membrane sides at 11 °C. In addition, two manometers (MEX3D820B15, Bourdon) measured the pressure at tube and shell sides yielding pressure different values close to 0 bar.

The red wine studied was Tempranillo, which corresponds to a black grape variety mainly grown in Spain, kindly provided by Bodegas Matarromera (Valbuena de Duero, Valladolid, Spain). OD tests were performed recirculating 250 mL of wine through the shell side of the membrane module at 74 mL·min⁻¹. Meanwhile, 125 mL of the extracting agent (deionized water) was fed at 40 mL·min⁻¹ to the tube side of the membrane module. Deionized water allowed to minimize the water transport across the membrane and therefore its extraction from wine and its potential transport to it, estimated in less than 0.1 v/v% decrease in the ethanol content by dilution with water. Both streams were continuously applied in a counter current configuration working at 11 °C to minimize the losses of aromas, especially esters. Flows and volumes were established in a previous publication where the influence of different variables in the operation of the OD was investigated [12]. OD experiments were performed by duplicate. After each experiment, the OD module was cleaned at 40–60 °C with a 0.5 wt/v% NaOH solution following a procedure previously described [12].

Pervaporation experimental setup

The PV setup consists of two steps, carrying out a first hydrophobic separation process (HFB-PV) followed by a hydrophilic one (HFL-PV). The HFB-PV separated ethanol from the OD waste, obtaining a permeate enriched in ethanol. Subsequently, this permeate was subjected to a step of dehydration with a hydrophilic membrane, obtaining an ethanol-rich stream as retentate. This scheme allowed the reuse of the retentate of the HFB-PV and the permeate of the HFL-PV as extracting agent in a next OD process.

As shown in Figure S1, two different membrane modules were used to place the PV membranes. Tubular membranes were coupled in a homemade stainless steel permeation module sealed with viton o-rings, while flat sheet membranes were placed in a stain-

less steel permeation module from Sartorius™. The driving force for the separation is the difference in partial pressures between both membrane sides, which was achieved by a Pfeiffer vacuum pump (MVP-040–2) connected to the permeate side.

In both types of PV, a flow of 15 mL·min⁻¹ was fed to the membrane module at atmospheric pressure, while the permeate vacuum pressure was controlled at 4 mbar by a needle valve and monitored with a pressure transducer connected to a digital display. The permeated vapor was condensed by means of two consecutive glass traps immersed in liquid nitrogen (–196 °C) dewar flasks and collected at fixed times, while the retentate stream was recycled back to the feed tank. Preliminary experiments, fed with water–ethanol synthetic solutions (5.3 wt% ethanol in HFB-PV and 40 wt% ethanol in HFL-PV), were performed to fix the optimum operation conditions and choose the best membranes in terms of PV flux and separation factor. Once the PV setup was validated with water–ethanol solutions, both PV steps were carried out feeding real solutions as above mentioned. Table 1 shows the experimental conditions applied in both PV tests. To obtain average values and standard deviations, each experiment under non steady state conditions was carried out twice (E1–E3, E6–E8), while in those under steady state three successive samples were taken at 3 h intervals (E4 and E5).

Membrane performance in PV was assessed based on the permeation flux (J , kg·m⁻²·h⁻¹) and the separation factor (α). The total PV flux was obtained at fixed time intervals from the following equation:

Table 1

PV experiments carried out with water–ethanol solutions. SIL, MOR1 and MOR2 and FAU are zeolite membranes of silicalite-1, mordenite and faujasite, respectively.

Exp	Membrane	Temperature [°C]	Feed [g]	Feed ethanol [wt%]
E1	SIL	40	100	5.3
E2	SIL	60	100	5.3
E3	PDMS	60	100	5.3
E4	MOR1	55	1000	40
E5	MOR1	75	1000	40
E6	MOR1	75	100	40
E7	MOR2	75	100	40
E8	FAU	75	100	40

$$J = \frac{\Delta W}{A_e \Delta t} \quad (1)$$

where ΔW (kg) is the variation of total mass in a given interval of time, Δt (h), and A is the effective membrane area (m^2). From ΔW and the corresponding concentrations of permeate samples, ethanol and water permeate fluxes were also obtained. The separation factor ($\alpha_{A/B}$) was calculated as follows:

$$\alpha_{A/B} = \frac{Y_A/Y_B}{X_A/X_B} \quad (2)$$

where X_A and X_B and Y_A and Y_B are the weight fractions of A (desired component) and B in the retentate and permeate sides, respectively. For the experiments carried out under steady state conditions (E4 and E5), $\alpha_{A/B}$ was calculated as an average of three runs with the same membrane once the steady state was reached. For non-steady state ones (E1-E3; E6-E8), $\alpha_{A/B}$ was obtained from each collected permeate along the experiment. Moreover, permeances (P_i) were calculated normalizing each individual flux by the driving force as follows:

$$P_i = \frac{j_i}{p_{i,R} - p_{i,P}} \quad (3)$$

$p_{i,R}$ and $p_{i,P}$ being the vapor pressures of component i in the retentate and permeate sides, respectively.

After each experiment, mass compositions of retentate and permeate were determined to calculate the recovery efficiency to ethanol. Finally, both OD and PV polymeric membranes were cleaned with pure ethanol at 60 °C for 8 h followed by drying overnight at 60 °C. As the silicalite-1 membrane suffered from fouling due to the presence of some organic compounds in the PV feeding, a calcination step was undergone in a furnace at 480 °C for 12 h with a heating rate of 0.5 °C \cdot min $^{-1}$.

Chromatographic analyses

In both processes (OD and PV), 1 mL volumes of the different streams were taken at constant time intervals to analyze their ethanol concentration. Methanol (HPLC grade, Scharlau) (20 μ L) was added to each sample as internal standard. An aliquot of this mixture (0.5 μ L) was injected to a gas chromatograph (7820A, Agilent Technologies) equipped with a Porapak Q80/100 column, 2 m \times 1.8 mm \times 2 mm, a thermal conductivity detector (TCD) and a flame ionization detector (FID). The injector worked at 250 °C in splitless mode with a ratio 1:100. Helium was used as carrier gas at a constant flow of 1 mL(STP) \cdot min $^{-1}$ and the temperature in the oven was fixed at 200 °C. After each experiment, the major volatile compounds in all wines were analyzed following a procedure previously reported based on gas chromatographic-flame ionization [57].

Results and discussion

Partial dealcoholization of red wine by membrane OD

Feed for the further PV setup was obtained from the partial dealcoholization of red wine (initial composition in Table S1) by OD, using deionized water as extracting agent. Under the previously mentioned experimental conditions, a 3 v/v% (2.5 wt%) ethanol decrease was achieved after 25 min. This means that 250 mL of wine feed (V_f) and 125 mL of water (V_s) were pumped to both sides of the membrane module. In these conditions, 125 mL of a stripping phase with a 5.3 wt% ethanol was produced in each OD run (corresponding to an ethanol osmotic pressure of 0.26 atm), while in the feed side the ethanol concentration was reduced from 14.0 to 11.2 v/v% (corresponding to a change in the ethanol osmotic

pressure from 0.56 to 0.45 atm). The difference in osmotic pressure of the main solute of wine (ethanol) between both membrane sides generates the needed driving force for the dealcoholization. In successive OD dealcoholization experiments, the water recovered from the pervaporation modules (125 mL, 0.4 wt% ethanol) was used instead of fresh, deionized water.

A total of 25 compounds were identified and quantified by gas chromatography in the starting wine and in the two dealcoholized wines (W_A and W_B , with fresh deionized water and recycled PV water, respectively). As expected, both wines W_A and W_B systematically have less content of aromas than the fresh wine. Hence, a loss of some volatile compounds is unavoidable due to the existence of favorable concentration gradients for these components between both membrane sides. Moreover, other factors such as volatility of each component, interaction with the wine matrix and affinity to the membrane material also have an impact on the loss of volatile compounds [12–15,18,19]. These compounds can be grouped in the following chemical families: alcohols, esters, acids, ketones, lactones and sulfur compounds. The behavior of each volatile compound (Fig. 2A) and of each chemical family (Fig. 2B) during OD adequately correlated with the corresponding Henry's constant (H^i) value (in water; values obtained from previous literature, see Table S2 [58]) using both stripping agents. The expected trend is the higher the H^i value of a given component i , the higher its water solubility and the lower its loss. This behavior has already been observed in recent studies, being consistent with the loss of components towards the stripping phase together with the ethanol [12–14,18,19].

As Fig. 2A depicts, all the aliphatic alcohols exhibit a similar behavior with an average loss of 26%, close to the ethanol loss (ca. 20%) in agreement with their close Henry's constant values (with an average value of 1.2 mol \cdot m $^{-3}$ \cdot Pa $^{-1}$). However, aromatic alcohols remained in wine after achieving the same degree of dealcoholization. The different behavior between both alcohol types (aliphatic and aromatic) is in agreement with the H^i for aromatic alcohols (18 mol \cdot m $^{-3}$ \cdot Pa $^{-1}$, Fig. 2B), supported by the π - π stacking interactions and that of the -OH groups with the rest of the wine components [59].

Concerning esters, the concentrations of those derived from straight chain fatty acids (ethyl esters -SC-) suffer a slightly higher average decrease (ca. 33%) than aliphatic alcohols (Fig. 2B). This agrees with their lowest overall average value of Henry's constant (0.022 mol \cdot m $^{-3}$ \cdot Pa $^{-1}$) (Fig. 2B). In addition, those derived from fermentation acids (ethyl esters -FA-; ethyl lactate and diethyl succinate) were the esters with the lowest loss (14% and 11%, respectively), in line with their higher Henry's constant values (17 and 4.0 mol \cdot m $^{-3}$ \cdot Pa $^{-1}$, respectively). Moreover, isoamyl acetate shows the highest concentration decrease (46%) in agreement with its small Henry's constant (0.021 mol \cdot m $^{-3}$ \cdot Pa $^{-1}$). In any event, these losses are lower than those previously reported by other authors [10,13,15] also using membrane techniques. This can be due to the low temperature applied here (11 °C) for the membrane OD.

Acids show a lower loss (17% in average) than alcohols and esters (Fig. 2B). This agrees with their higher Henry's constant values (8.7 mol \cdot m $^{-3}$ \cdot Pa $^{-1}$), although the most volatile carboxylic acid, acetic acid, shows a ca. 30% loss, close to the values corresponding to aliphatic alcohols.

Acetoin, methionol and δ -butyrolactone were also studied. Acetoin, shows a relatively small loss, in agreement with its Henry's constant value as can be seen in Fig. 2B. The concentrations of methionol, a sulfur compound, and δ -butyrolactone, a lactone, were not significantly affected by the dealcoholization process, as expected from their high Henry's constant values shown (100 and 190 mol \cdot m $^{-3}$ \cdot Pa, respectively).

In summary, the aroma losses reported here and the profile of each chemical family were basically in agreement with the litera-

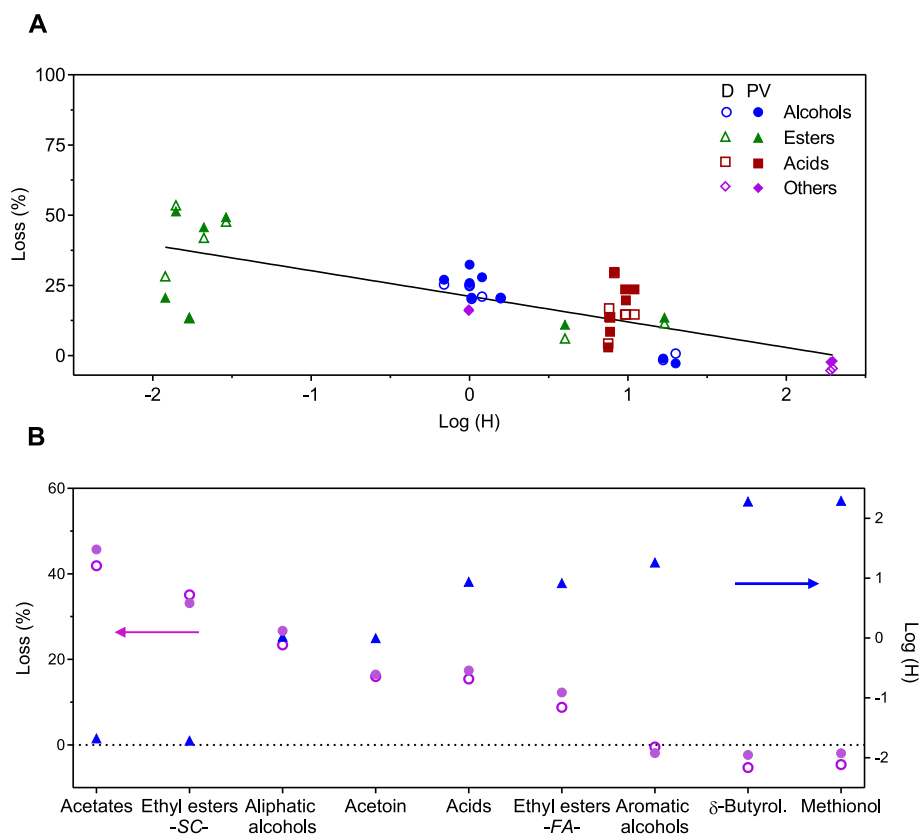


Fig. 2. A) Losses of volatile compounds as a function of Henry's constant ($\log H^I$ with H^I in $\text{mol}\cdot\text{m}^{-3}\cdot\text{Pa}^{-1}$). B) Average losses and $\log H^I$ values of volatile compounds grouped by chemical families. In A and B, solid and open symbols correspond to OD with fresh (D) and recycled water (PV), respectively. SC and FA in B refer to ethyl esters from straight chain fatty and from fermentation acids, respectively.

ture, suggesting that the experimental conditions used in this work, advantageous due to the low temperature applied, are appropriate to accomplish the dealcoholization by OD [11,15,60].

Finally, the OD polypropylene membrane module used in this work was discontinuously operated along ca. 3 years accumulating 26 h of red wine dealcoholization, 7 h of water–ethanol dealcoholization, ca. 15 h of 0.5 wt.% NaOH cleaning at 40–60 °C and almost 8 days under vacuum (4 mbar). Despite this, the module showed reproducible dealcoholization results, proving its stability.

Hydrophobic PV of water–ethanol solutions

To study the performance of the PV setup (see Fig. 1) and establish the best membrane for each step, several preliminary experiments were carried out feeding different water–ethanol solutions for their dealcoholization (with hydrophobic membrane) or dehydration (with hydrophilic membrane). In case of experiments done under non-steady state (E1–E3; E6–E8), the composition changed notably during the experiments and, as a result, so did the PV flux and separation factor. In these conditions, PV flux and separation factor were obtained from each collected permeate along the experiments. In any event, the runs carried out correspond to batch experiments accounting for relatively small amounts of wine and the different PV solutions to treat. However, it is expected that the results gathered from them help establish the conditions for a suitable continuous industrial process.

The first PV step for the treatment of the OD extracting stream is its dealcoholization by HFB-PV. A synthetic ethanol–water mixture with the same composition as the OD extracting stream (ethanol content 5.3 wt%) was submitted to PV with hydrophobic membranes. Membranes used for this purpose were made of

hydrophobic PDMS (membrane PDMS) and zeolite silicalite-1 (membrane SIL). Experiments were stopped when a reference content of alcohol in retentate around of 0.4 wt% was reached, as a compromise between decreasing the ethanol content in the extracting phase and the fact that an excessive experiment time may dilute the permeate stream, hindering the next PV stage (since an ethanol content close to 40 wt% is required for HFL-PV).

In order to select the most favorable experimental conditions for HFB-PV, several experiments were carried out to determine the optimum temperature and membrane type. Table 2 and Fig. 3 show the results corresponding to these experiments. In addition, the average values of total permeate weight collected of each experiment are summarized in Table S3. As shown in Fig. 3A, all HFB-PV experiments were carried out under non-steady state conditions, the driving force for ethanol permeation decreasing and leading to a reduction in the ethanol permeation flux with experiment time. As a result, ethanol concentration in the retentate side diminished along the experiments (see Fig. 3B).

As can be seen in Fig. 3B, the degree of ethanol removal (considering the above-mentioned ~ 0.4 wt% limit) was successfully achieved at both temperatures of 40 and 60 °C working with membrane SIL. However, a lower total flux was shown by membrane SIL at 40 °C (Table 2), meaning a longer time to reach the target ethanol content in retentate of 0.4 wt%. Besides, the temperature did not seem to influence on the total PV flux tendency, remaining it approximately constant along the experiment at both temperatures (Figure S2). Thus, working at 60 °C allowed to obtain a higher PV flux for ethanol than for water (0.46 and 0.32 $\text{kg}\cdot\text{m}^{-2}\cdot\text{h}^{-1}$, respectively) at the beginning of the HFB-PV experiments. This led to the recovery of a higher amount of retentate (87% at 60 °C; 76% at 40 °C) with an ethanol concentration around 0.4 wt%. This low ethanol concentration in the retentate stream will con-

Table 2

Pervaporation with hydrophobic membranes (HFB-PV) at 40 and 60 °C. Ethanol in the feed was 5.3 ± 0.1 wt%. Ethanol concentrations of retentate and permeate and total fluxes determined at the end of each experiment.

Membrane	Run	Temperature [°C]	Ethanol content [wt%]		$\alpha_{\text{ethanol/water}}$ [-]	Total flux [$\text{kg}\cdot\text{m}^{-2}\cdot\text{h}^{-1}$]
			Retentate	Permeate		
SIL	E1	40	0.46 ± 0.0	23 ± 3	18.0 ± 4.8	0.32 ± 0.0
SIL	E2	60	0.40 ± 0.1	36 ± 1	37.4 ± 4.5	0.69 ± 0.1
PDMS	E3	60	0.94 ± 0.0	12 ± 0	6.0 ± 0.3	1.7 ± 0.0

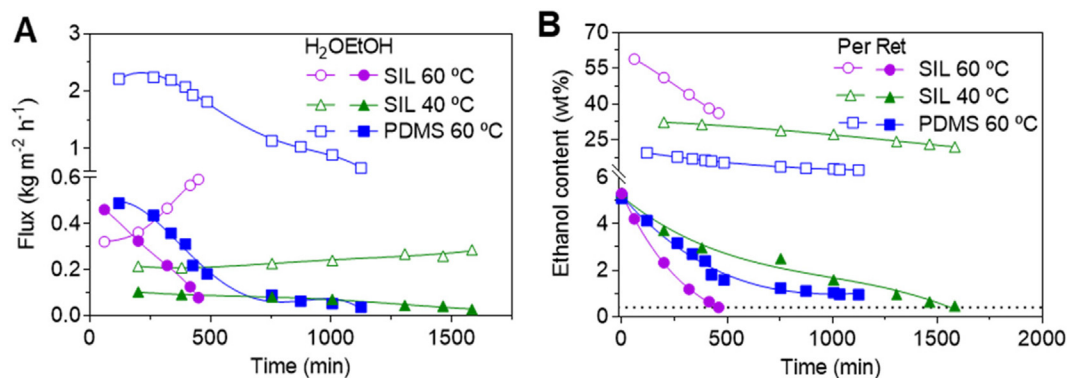


Fig. 3. HFB-PV of 100 g of a water–ethanol solution with 5.3 ± 0.1 wt% of ethanol. A) Ethanol (closed symbols) and water (open symbols) fluxes as a function of time. B) Ethanol content as a function of time in retentate (closed symbols) and permeate (open symbols); the dashed straight line corresponds to the 0.4 wt% ethanol concentration. The continuous lines are guides to the eye.

tribute to generate the stripping agent for reuse in OD. Under these conditions and as shown in Fig. 3B, a permeate with a higher ethanol content was obtained at 60 °C (36 wt%) than at 40 °C (23 wt%), the first being closer to the ethanol concentration fixed as an adequate feed (40 wt%) for the next HFL-PV step. In consequence, the optimum temperature to carry out HFB-PV was set at 60 °C.

As can be seen in Fig. 3A, membrane PDMS exhibits the highest total flux value (Table 2), decreasing sharply with time until reaching values close to those of membrane SIL at the same temperature (60 °C). However, this higher total flux obtained with PDMS in comparison with that of SIL did not cause the expected reduction in ethanol content in the retentate, due to the lower ratio between ethanol and water fluxes shown. This is in agreement with a higher separation factor of membrane SIL with respect to membrane PDMS as shown in Table 2. In fact, the PDMS ethanol PV flux diminished over time until reach a very small value ($0.04 \text{ kg}\cdot\text{m}^{-2}\cdot\text{h}^{-1}$ after 1000 min), while the water flux remained at a considerable high level ($0.65 \text{ kg}\cdot\text{m}^{-2}\cdot\text{h}^{-1}$ after 1000 min). This prevented from achieving the degree of dealcoholization proposed, obtaining an alcohol concentration of 0.94 wt% in the retentate and generating an insufficient ethanol concentration in the permeate of 12 wt% (Table 2). In summary, membrane SIL is considered as the best to carry out the hydrophobic separation and decrease the alcohol concentration in the retentate below 0.4 wt%, the optimum temperature being set at 60 °C to obtain an alcohol rich permeate in a short time (Fig. 3B). In these conditions, an ethanol/water separation factor of up to 37.4 (as compared to 6.0 with PDMS) with an ethanol flux of $0.69 \text{ kg}\cdot\text{m}^{-2}\cdot\text{h}^{-1}$ were obtained (Table 2). In any event, the PV flux and separation factor values are in agreement with those achieved with similar hydrophobic membranes applied generally to higher concentration feeds [61].

Another interesting information can be gathered from the PDMS membranes. As a preliminary work, membrane PDMS was used to evaluate the PV performance from different feeds, from a synthetic ethanol–water solution (13 wt% ethanol concentration) to red wine full of aromas (13 wt% ethanol concentration). A summary of these results is shown in Table S4. No significant

differences in ethanol/water separation factors were observed as a function of feed concentration, while a decrease of PV flux was observed from $0.9 \text{ kg}\cdot\text{m}^{-2}\cdot\text{h}^{-1}$ (ethanol–water solution) to $0.6 \text{ kg}\cdot\text{m}^{-2}\cdot\text{h}^{-1}$ (red wine) in agreement with some dissolution of the wine aromas on the PDMS membrane slowing the PV flux. In any event, the concentration in volatile compounds in the OD waste is much lower than that in wine, as will be shown below.

Hydrophilic PV of water–ethanol solutions

A synthetic hydroalcoholic solution with 40 wt% ethanol (fixed as an adequate concentration to carry out the dehydration process) was used as feed for the second HFL-PV step with the aim of increasing the ethanol concentration and obtaining a water-like permeate that could be used as stripping agent in further OD. Membranes used for this purpose were made of hydrophilic zeolites mordenite (membranes MOR1 and MOR2) and faujasite (membrane FAU). These zeolite membranes prepared on tubular mullite supports have shown very good performance when dehydrating organic compounds or separating the most polar compound in a given organic mixture [62].

Given the important effect of temperature observed on the hydrophobic separation, this parameter was first studied to enhance the HFL-PV. Membrane MOR1, whose results are summarized in Table 3, was tested at 55 and 75 °C at steady state conditions (i.e. ethanol concentration at feed or retentate side approximately constant at 40 wt%). As the temperature increased so did the total PV flux and the separation factor, which is in agreement with a previous work using hydrophilic zeolites where the water flux was activated in this temperature range [63]. This allowed to fix 75 °C as the optimum temperature to carry out the HFL-PV.

Once fixed the optimum temperature to carry out the HFL-PV, Table 4 shows the comparison between mordenite and faujasite membranes operating under non-steady state conditions to emulate the dehydration of the permeate from HFB-PV. In addition, Fig. 4 depicts the evolution of the HFL-PV fluxes and the water

retentate and permeate concentrations as a function of time for each membrane, under non-steady state. Sooner (membrane FAU because of its high water PV flux, see Fig. 4A) or later (membranes MOR1 and MOR2) the retentate reached in all cases an ethanol concentration over 99 wt%, as shown in Fig. 4B related to the low water concentration achieved at a certain operation time. In this sense, membrane FAU allowed a faster decrease in the water concentration, according to its higher total PV flux ($3.4 \text{ kg}\cdot\text{m}^{-2}\cdot\text{h}^{-1}$) than those of the two mordenite membranes (ca. $1.1\text{--}1.2 \text{ kg}\cdot\text{m}^{-2}\cdot\text{h}^{-1}$), reaching the bioethanol target concentration of 99% 3 times faster. However, the high total flux shown by FAU did not allow to reuse the permeate generated as stripping phase in the OD, due to the high ethanol concentration remained (18.7 wt%), unsuitable for the stripping phase. This is in agreement with the low water/ethanol separation factor of 21.2 for FAU as compared to the much higher values for MOR of up to 7225, see runs E8 and E7 in Table S3.

The previous results can be explained by the evolution of water and ethanol fluxes that permeate through membrane FAU along time. As observed in Fig. 4A, the water flux started at a higher value ($4.6 \text{ kg}\cdot\text{m}^{-2}\cdot\text{h}^{-1}$) than that of the ethanol flux ($0.26 \text{ kg}\cdot\text{m}^{-2}\cdot\text{h}^{-1}$), generating a permeate with a 5.7 wt% ethanol concentration. Nevertheless, it rapidly became lower than the ethanol flux, meaning that only 65% of total ethanol in the feed was recovered as bioethanol. Besides, although no important differences in permeance of mordenite membranes were observed (Table 4), membrane MOR1 required more time to reach the same dehydration degree. This result can be explained by the similar water flux of both membranes but with a less ethanol flux of MOR2 (Fig. 4B). Therefore, permeates obtained with MOR2 working at 75°C are more suitable to be reused as stripping phase in OD.

Finally, as shown in Figure S3, regarding the experiments in Tables 2 and 4, water and ethanol pervaporation permeances were calculated according to equation (3). Even though the discussion along the work has been done in terms of fluxes, it is true that these values are not only function of the intrinsic properties of the membranes used (in this case very different since both hydrophobic and hydrophilic membranes have been applied), but also depend on the operating conditions (feed concentration and temperature and vapor pressure driving force) [64]. The presentation of permeances may facilitate the comparison of the current work results with those obtained under different pervaporation conditions but with the same mixtures studied here.

PV of extracting solutions

As compared to SIL membranes with a much higher Si/Al ratio [53], MOR and FAU membranes are characterized by a low Si/Al ratio [54,55]. This low Si/Al ratio allows the introduction of compensation cations in the zeolite framework turning it hydrophilic. It is generally admitted that non-zeolite pores and structural defects in zeolite membranes have a stronger effect on hydrophobic membranes than on hydrophilic ones because of the presence of silanol groups on the zeolite surface which favors the PV of polar compounds [47]. This explains the much higher separation factors achieved with MOR membranes than with SIL membranes, both being the best performing hydrophobic and hydrophilic mem-

branes to be used for the PV of OD extracting solutions in this section.

The hydrophobic-hydrophilic PV, equipped with the membranes chosen in the present study (SIL as a hydrophobic membrane and MOR2 as a hydrophilic one), was tested using OD waste as feed as shown in Table 5. In what concerns the ethanol recovery, carrying out the global PV process under the optimum conditions, HFB-PV allowed to recover 92% of the ethanol removed from red wine by membrane OD. This ethanol (36 wt%) was fed to the subsequent HFL-PV where in turn 98% of ethanol was retained as dehydrated ethanol (bioethanol) with MOR2. This bioethanol is more than 99 wt% in ethanol, having overcome the azeotropic composition. It is interesting to note that the alcohol concentration in the permeate of the hydrophobic PV is high enough as to avoid the need of a thermal process of ethanol concentration in between [65]. In summary, from a reduction of 3 v/v% in the alcoholic degree of wine, the hydrophobic-hydrophilic PV setup allowed to recover as bioethanol 88% of the ethanol removed from the wine (percentage calculated by total mass balance). In addition, no significant major differences in the membrane SIL performance were found when facing a water-ethanol solution or OD wastewater with traces of organic compounds (see Table 6). This suggests that the ethanol recovery from OD waste is probably easier than from fermentation broths [66]. MOR2 showed a comparable performance with both feeds too, confirming the high stability reported for this zeolite membrane [55,67].

Despite having selected membrane SIL as the optimum membrane based on the results obtained from HFB-PV experiments with water-ethanol solutions, both hydrophobic membranes PDMS and SIL were fed with OD wastewater. This was mainly due to the fact that a fouling phenomenon was observed in previous experiments with solutions enriched (aroma concentrate, as compared to the OD wastewater, see Table 6) in some selected aroma compounds using membrane SIL. However, this effect was not observed with the low PV performance membrane PDMS (not shown).

The study of the stability of the membrane PV operation when dealing with realistic mixtures is of great importance. Abounding on the silicalite-1 membrane performance, Fig. 5 and Table S5 show the history of membrane SIL submitted to 174 h of accumulated experiments under different conditions. Experiments 1, 2, 16 and 17 were carried out at 40°C with a PV flux of ca. $0.3 \text{ kg}\cdot\text{m}^{-2}\cdot\text{h}^{-1}$, runs 3–8, 14, 15 and 18–21 were at 60°C with higher PV flux in the $0.6\text{--}0.7 \text{ kg}\cdot\text{m}^{-2}\cdot\text{h}^{-1}$ range regardless of using water-ethanol solutions or OD wastewater (with traces of aromas, as shown in Table 6). Nevertheless, experiments 9 and 10 with an aroma concentrate feed (at much higher concentrations than those observed in the OD wastewater) accelerated the fouling of the hydrophobic zeolite membrane provoking a huge diminishing of its PV flux. This was not recovered during next runs 11–13 with water-ethanol and required of a calcination stage at 480°C for 12 h to retrieve the initial performance of the membrane (from run 14).

To complete the discussion about the PV membrane stability, Table 7 summarizes the histories of the four PV membrane types applied in this work. In case of PDMS, a different membrane sample was used for each different feed, while membranes SIL and MOR (in this case with two samples) were intensively exposed to different PV conditions regarding temperature and feed con-

Table 3

Pervaporation with hydrophilic membranes (HFL-PV) under steady state conditions at two different temperatures. Ethanol in the feed was $40 \pm 0.1 \text{ wt}\%$.

Membrane	Run	Temperature [$^\circ\text{C}$]	Ethanol content [wt%]		$\alpha_{\text{water/ethanol}}$ [-]	Total flux [$\text{kg}\cdot\text{m}^{-2}\cdot\text{h}^{-1}$]
			Retentate	Permeate		
MOR1	E4	55	40 ± 0.5	3.7 ± 0.3	17.4 ± 1.5	0.69 ± 0.0
MOR1	E5	75	40 ± 0.7	2.1 ± 0.3	39.1 ± 3.6	1.2 ± 0.0

Table 4

Pervaporation with hydrophilic membranes (HFL-PV) under non-steady state conditions at 75 °C. Ethanol in the feed was 40 ± 0.1 wt%. Ethanol concentrations of retentate and permeate and total PV flux obtained at the end of each experiment.

Membrane	Run	Ethanol content [wt%]		$\alpha_{\text{water/ethanol}}$ [-]	Total flux [$\text{kg m}^{-2} \text{h}^{-1}$]
		Retentate	Permeate		
MOR1	E6	>99	3.1 ± 0.4	736 ± 296	1.1 ± 0.2
MOR2	E7	>99	< 0.2	7225 ± 2009	1.2 ± 0.2
FAU	E8	>99	19 ± 4	21.2 ± 7.5	3.4 ± 0.4

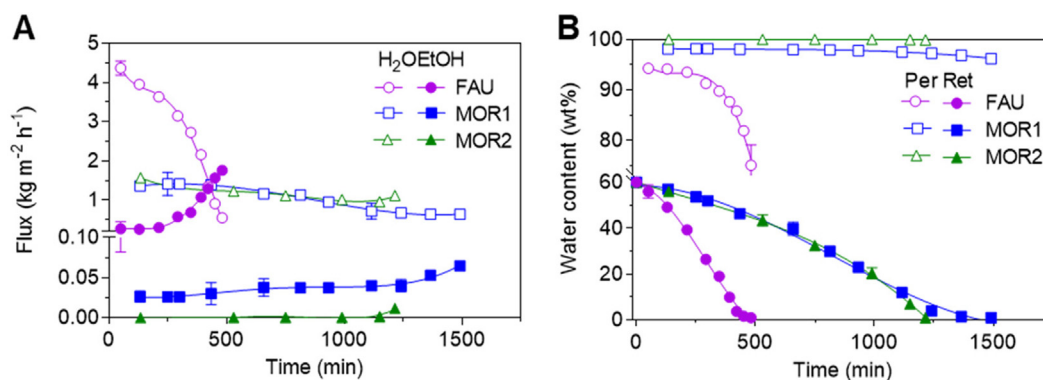


Fig. 4. HFL-PV results feeding 100 g of a water–ethanol solution with 40 ± 0.1 wt% of ethanol. A) Ethanol (closed symbols) and water (open symbols) fluxes as a function of time. B) Water content as a function of time in retentate (closed symbols) and permeate (open symbols). The continuous lines are guides to the eye.

Table 5

PV performance with best hydrophobic (silicalite-1, SIL, ethanol/water separation factor) and hydrophilic (mordenite, MOR2, water/ethanol separation factor) membranes.

	Feed	Ethanol content [wt%]		Time (min)	Ethanol recovery [%]	Separation factor [-]	Total flux [$\text{kg m}^{-2} \text{h}^{-1}$]
		Initial (feed)	Final (retentate)				
HFB-PV	Water-ethanol solution (100 g)	5.3	0.4	460	93	37.4 ± 4	0.69 ± 0.1
	OD waste (125 g)	5.2	0.4	550	92	36 ± 4	0.72 ± 0.0
HFL-PV	Water-ethanol solution (100 g)	40	>99	1215	99	7225 ± 2009	1.2 ± 0.2
	Permeate from HFB-PV (17 g)	36	>99	300	98	6918 ± 728	1.2 ± 0.2

Table 6

Compositions of selected aroma compounds in red wine, aroma concentrate (balanced with 50%/50% ethanol/water) and OD wastewater as determined by chromatography.

Aroma	Red wine [mg L^{-1}]	Aroma concentrate [mg L^{-1}]	OD wastewater [mg L^{-1}]
Isoamyl acetate	0.44 ± 0.07	3.5 ± 0.17	0.15 ± 0.03
Ethyl acetate	56 ± 3	5.7 ± 0.2	14.1 ± 0.6
Ethyl lactate	61 ± 4	3.7 ± 0.3	4.8 ± 0.5
Isoamyl alcohol	222 ± 5	154 ± 7	103 ± 1.3
β -Phenylethanol	32.0 ± 0.6	10 ± 0.2	0.79 ± 0.29
Acetic acid	429 ± 40	0.43 ± 0.07	0.68 ± 0.07
Hexanoic acid	1.8 ± 0.0	3.3 ± 0.08	0.11 ± 0.00
γ -Butyrolactone	17.0 ± 0.6	4.0 ± 0.4	0.36 ± 0.00

centration, as seen above for membrane SIL, demonstrating their high stability and robustness. Hydrophilic membrane FAU was studied only with water–ethanol solutions due to its worse performance in terms of separation factor as compared to membranes MOR.

As shown in Table S6, these results agree with previous work in which the ethanol–water mixture was separated by hydrophobic PV with a PDMS membrane (working at similar levels of PV flux and separation factor in case of membrane PDMS but much lower than those achieved with the silicalite-1 membrane) generating a permeate with 80 wt% ethanol [50]. This permeate was submitted

to secondary PV with carboxymethyl cellulose (CMC) membrane giving rise to 99 wt% water. Similar strategy was used with PDMS/PVA (polyvinyl alcohol) hydrophobic/hydrophilic membranes to obtain 99 wt% isobutanol from a 2 wt% aqueous isobutanol solution [51]. Even if the hydrophilic PV with the PVA membrane yielded a very low water/alcohol separation factor, that reported with the CMC membrane was comparable to those achieved in this work with the MOR membranes but with considerably lower PV flux: below 0.15–0.2 $\text{kg m}^{-2} \text{h}^{-1}$ at 25–30 °C with both CMC and PVA membranes. This highlights the advantages of the zeolite membranes, which are more stable, in the case of

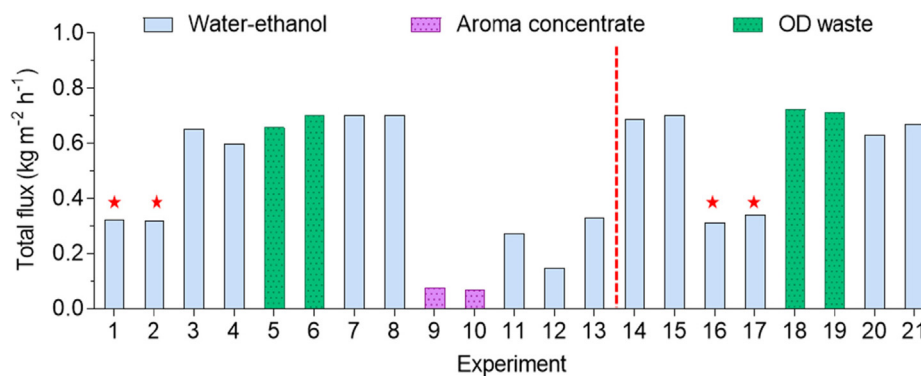


Fig. 5. Total PV flux for 21 experiments carried out with membrane SIL at 60 °C, except in those marked with a star, carried out at 40 °C. Total accumulated time: 174 h. The vertical red line indicates the calcination of the membrane at 480 °C.

Table 7

Experiments carried out with each membrane under several experimental conditions. W/E means water–ethanol solutions with an ethanol concentration of 1–5 wt%, aroma/W/E has the concentration shown in Table 6.

Membrane	Samples	Range of temperature [°C]	Time under stream [h]	Feed	Activation treatment
PDMS	4	30–60	89	W/E; wine; OD waste; aroma/W/E	-
SIL	1	40–60	174	W/E; OD waste; aroma/W/E	480 °C, 12 h
MOR	2	55–75	100	W/E; OD waste treated	-
FAU	1	75	16	W/E	-

silicalite-1 able to withstand a thermal reactivation treatment at 480 °C and also to perform with higher alcohol/water separation factors than the PDMS membranes, and much more permeable in the case of the hydrophilic membranes.

Partial dealcoholization of red wine with recycled water from membrane OD

Once both PV steps were optimized and validated with the water-rich volume generated in the membrane OD performed with fresh water, membrane OD was carried out with recycled water, constituted by combining the retentate of the hydrophobic PV with the permeate of the hydrophilic PV. This recycled water was used as extracting solution in a new membrane OD experiment, allowing a reduction in the water consumption associate to OD by 99%, from 0.5 to less than 0.005 liter of water per liter of wine (see Fig. 1), and giving rise to an analogous partially dealcoholized wine, in terms of contents of aroma compounds (see Fig. 2), than when using fresh deionized water. Indeed, together with the production of bioethanol, this is the main achievement of this work, thus demonstrating the saving of water during the whole operation of partial dealcoholization of wine without affecting its aroma profile as compared to the OD using fresh water.

In fact, in most cases the losses of aromas are comparable, within the experimental error, reusing the PV water (see W_B in Table S1) and applying fresh water (W_A). This allows to confirm that the reuse of water for the OD operation is an acceptable option from the separation point of view. It is worth mentioning that acids did show a slightly higher retention in wine when PV water was used as stripping stream. This can be due to the fact that PV water could include traces of some components, especially those that show a higher polarity, decreasing their driving force for the OD process.

These results demonstrate the feasibility of the approach carried out in this work where the OD wastewater is converted in bioethanol and the remaining water is reused for new OD. This agrees with previous LCA carried out on several common partial dealcoholization techniques, including membrane OD applied to wine, demonstrating that the high consumption of natural resources can be reversed by valorizing the wastewater [52], as done in this work by PV. Moreover, OD has other inherent advantages, since it can be done at a relatively low temperature (11 °C in this work) as compared, for instance, to the widely used spinning cone column treatment (working at 30 °C) [6], consequently affecting less the properties of wine.

Conclusions

Membrane osmotic distillation (OD) technology was applied to carry out a partial dealcoholization of red wine using a polypropylene hollow fiber membrane module. For a more sustainable process, OD was combined with hydrophobic-hydrophilic pervaporation (PV) carried out on the OD wastewater (only 5.3 wt% ethanol) allowing both the production of bioethanol and the recycle of water for the OD operation. In addition, the following conclusions can be gathered from this study:

- Preliminary PV experiments with ethanol–water solutions demonstrated the suitability of hydrophobic silicalite-1 (over polymeric PDMS) and hydrophilic mordenite (over faujasite) zeolite membranes to carry out the respective hydrophobic and hydrophilic PV.
- Constituting an illustrative example of process intensification, the combination of OD with a sequential hydrophobic-hydrophilic PV process, mainly based, respectively, on zeolite membranes of silicalite-1 (working at 60 °C) and mordenite (at 75 °C) adds value to the water-rich waste product from

OD, transformed into recycled water with ca. 0.4 wt% ethanol, constituted by combination of the retentate of the hydrophobic pervaporation with the permeate of the hydrophilic pervaporation, and bioethanol (ca. 99 wt.% ethanol), i.e. the retentate of the hydrophilic pervaporation.

- The recycled water was used as extracting solution in a new membrane OD operation, giving rise to analogous partially dealcoholized wine, in terms of contents of aroma compounds, than that achieved when using fresh deionized water. This strategy reduced the water consumption to practically zero in the whole process, which is of paramount importance to validate the industrial potential of membrane OD to dealcoholize wine.
- Finally, 88% of the ethanol removed from wine could be recycled into sustainable bioethanol, alternative to fossil fuels, confirming that the global process frames within the rule of the three Rs of reuse, recycle and reduce.

Declaration of Competing Interest

The authors declare that they have no known competing financial interests or personal relationships that could have appeared to influence the work reported in this paper.

Acknowledgements

Grant RTC-2017-6360 funded by MCIN/AEI/10.13039/501100011033 and by ERDF. A way of making Europe.

Appendix A. Supplementary data

Supplementary data to this article can be found online at <https://doi.org/10.1016/j.jiec.2023.02.024>.

References

- [1] N.H. Mermelstein, *IFT*. 54 (2000) 89.
- [2] A.L. Robinson, S.E. Ebeler, H. Heymann, P.K. Boss, P.S. Solomon, R.D. Trengove, *J. Agric. Food Chem.* 57 (2009) 10313–10322.
- [3] B. Pineau, J.C. Barbe, C. Van Leeuwen, D. Dubourdieu, *J. Agric. Food Chem.* 55 (2007) 4103–4108.
- [4] M.A. Olego, F. Visconti, M.J. Quiroga, J.M. de Paz, E. Garzón-Jimeno, *Spanish J. Agric. Res.* 14 (2016).
- [5] S. Dequin, J.-L. Escudier, M. Bely, J. Noble, W. Albertin, I. Masneuf-Pomarède, P. Marullo, J.-M. Salmon, J.M. Sablayrolles, *OENO One*. 51 (2017) 205–214.
- [6] L.M. Schmidtke, J.W. Blackman, S.O. Agboola, *J. Food Sci.* 77 (2012) R25–R41.
- [7] M. Catarino, A. Mendes, L.M. Madeira, A. Ferreira, *Sep. Sci. Technol.* 42 (2007) 3011–3027.
- [8] M. Catarino, A. Mendes, *Innov. Food Sci. Emerg. Technol.* 12 (2011) 330–337.
- [9] F.E. Sam, T.Z. Ma, R. Salifu, J. Wang, Y.M. Jiang, B. Zhang, S.Y. Han, *Foods*. 10 (2021) 2498.
- [10] L. Liguori, P. Russo, D. Albanese, M. Di Matteo, *Food Chem.* 140 (2013) 68–75.
- [11] O. Corona, L. Liguori, D. Albanese, M. Di Matteo, L. Cinquanta, P. Russo, *Eur. Food Res. Technol.* 245 (2019) 2601–2611.
- [12] J. Esteras-Saz, Ó. de la Iglesia, C. Peña, A. Escudero, C. Téllez, J. Coronas, *Sep. Purif. Technol.* 270 (2021).
- [13] L. Liguori, D. Albanese, A. Crescitelli, M. Di Matteo, P. Russo, *J. Food Sci. Technol.* 56 (2019) 3707–3720.
- [14] L. Liguori, P. Russo, D. Albanese, M. Di Matteo, *Food Bioprocess Technol.* 6 (2013) 2514–2524.
- [15] M.T. Lisanti, A. Gambuti, A. Genovese, P. Piombino, L. Moio, *Food Bioprocess Technol.* 6 (2013) 2289–2305.
- [16] L. Liguori, G. De Francesco, P. Russo, D. Albanese, G. Perretti, M. Di Matteo, *Chem. Eng. Trans.* 43 (2015) 13–18.
- [17] G. De Francesco, O. Marconi, V. Sileoni, G. Freeman, E.G. Lee, S. Floridi, G. Perretti, *J. Food Sci. Technol.* 58 (2021) 1488–1498.
- [18] N. Diban, V. Athes, M. Bes, I. Souchon, *J. Memb. Sci.* 311 (2008) 136–146.
- [19] N. Diban, A. Arruti, A. Barceló, M. Puxeu, A. Urriaga, I. Ortiz, *Innov. Food Sci. Emerg. Technol.* 20 (2013) 259–268.
- [20] A. Cassano, C. Conidi, E. Drioli, *J. Memb. Sci. Res.* 6 (2020) 304–318.
- [21] P. García-Herreros, J.M. Golmez, I.D. Gil, G. Rodríguez, *Ind. Eng. Chem. Res.* 50 (2011) 3977–3985.
- [22] S. Karimi, R.R. Karri, M. Tavakkoli Yarak, J.R. Koduru, *Environ. Chem. Lett.* 19 (2021) 2873–2890.
- [23] M. Balat, *Energy Convers. Manag.* 52 (2011) 1479–1492.
- [24] B.D. Solomon, J.R. Barnes, K.E. Halvorsen, *Biomass and Bioenergy*. 31 (2007) 416–425.
- [25] M.N. Salimi, S.E. Lim, A.H.M. Yusoff, M.F. Jamlos, *J. Phys. Conf. Ser.* 908 (2017).
- [26] M. Irfan, M. Nadeem, Q. Syed, *J. Microbiol.* 45 (2014) 457–465.
- [27] S.B. Jamaldeen, P.B. Saynik, V.S. Moholkar, A. Goyal, *Bioresour. Technol. Reports*. 13 (2021).
- [28] K.M. Harinikumar, R.L. Kudahettige-Nilsson, A. Devadas, M. Holmgren, A. Sellstedt, *Biofuels*. 11 (2020) 607–613.
- [29] Y. Ai, S. Feng, Y. Wang, J. Lu, M. Sun, H. Hu, Z. Hu, R. Zhang, P. Liu, H. Peng, Y. Wang, L. Cao, T. Xia, L. Peng, *Ind. Crops Prod.* 173 (2021).
- [30] Ó.J. Sánchez, C.A. Cardona, *Bioresour. Technol.* 99 (2008) 5270–5295.
- [31] R.J. Bothast, M.A. Schlicher, *Appl. Microbiol. Biotechnol.* 67 (2005) 19–25.
- [32] G. Fischer, S. Prieler, H. van Velthuizen, G. Berndes, A. Faaij, M. Londo, M. de Wit, *Biomass and Bioenergy*. 34 (2010) 173–187.
- [33] E.B. Belal, *Braz J Microbiol.* 44 (2013) 225–234.
- [34] S. Banerjee, R. Sen, R.A. Pandey, T. Chakrabarti, D. Satpute, B.S. Giri, S. Mudliar, *Biomass and Bioenergy*. 33 (2009) 1680–1686.
- [35] J.C. Solarte-Toro, J.M. Romero-García, J.C. Martínez-Patiño, E. Ruiz-Ramos, E. Castro-Galiano, C.A. Cardona-Alzate, *Renew. Sustain. Energy Rev.* 107 (2019) 587–601.
- [36] C.A. Cardona Alzate, O.J. Sánchez Toro, *Energy*. 31 (2006) 2447–2459.
- [37] A. Ghofer, T. Kokugan, *Biochem. Eng. J.* 18 (2004) 235–238.
- [38] M. Gavahian, P.E.S. Munekata, I. Es, J.M. Lorenzo, A. Mousavi Khaneghah, F.J. Barba, *Green Chem.* 21 (2019) 1171–1185.
- [39] J.H.B. Jaimes, M.E.T. Alvarez, J.V. Rojas, R.M. Filho, *Chem. Eng. Trans.* 38 (2014) 139–144.
- [40] V. Van Hoof, L. Van den Abeele, A. Buekenhoudt, C. Dotremont, R. Leysen, *Sep. Purif. Technol.* 37 (2004) 33–49.
- [41] Y. Huang, R.W. Baker, L.M. Vane, *Ind. Eng. Chem. Res.* 49 (2010) 3760–3768.
- [42] P.D. Chapman, T. Oliveira, A.G. Livingston, K. Li, *J. Memb. Sci.* 318 (2008) 5–37.
- [43] C.L. Hsueh, J.F. Kuo, Y.H. Huang, C.C. Wang, C.Y. Chen, *Sep. Purif. Technol.* 41 (2005) 39–47.
- [44] S.H. Chen, R.M. Liou, C.S. Hsu, D.J. Chang, K.C. Yu, C.Y. Chang, *J. Memb. Sci.* 193 (2001) 59–67.
- [45] B. Bolto, M. Hoang, Z. Xie, *Chem. Eng. Process. Process Intensif.* 50 (2011) 227–235.
- [46] J. Coronas, J. Santamaría, *Sep. Purif. Rev.* 28 (1999) 127–177.
- [47] T.C. Bowen, R.D. Noble, J.L. Falconer, *J. Memb. Sci.* 245 (2004) 1–33.
- [48] A.J. Toth, A. Andre, E. Haaz, P. Mizsey, *Sep. Purif. Technol.* 156 (2015) 432–443.
- [49] A. Andre, T. Nagy, A.J. Toth, E. Haaz, D. Fozzer, J.A. Tarjani, P. Mizsey, *J. Clean. Prod.* 187 (2018) 804–818.
- [50] F.U. Nigiz, N. Durmaz Hilmioglu, *Energ. Source Part A* 38 (2016) 3348–3353.
- [51] M. Omidali, A. Raisi, A. Aroujalian, *Chem. Eng. Process. Process Intensif.* 77 (2014) 22–29.
- [52] M. Margallo, R. Aldaco, A. Barceló, N. Diban, I. Ortiz, A. Irabien, *Sustain. Prod. Consum.* 2 (2015) 29–39.
- [53] Y. Morigami, M. Kondo, J. Abe, H. Kita, K. Okamoto, *Sep. Purif. Technol.* 1–3 (2001) 251–260.
- [54] L. Qiu, I. Kumakiri, K. Tanaka, X. Chen, H. Kita, *J. Chem. Eng. Japan*. 50 (2017) 345–350.
- [55] M.H. Zhu, S.L. Xia, X.M. Hua, Z.J. Feng, N. Hu, F. Zhang, I. Kumakiri, Z.H. Lu, X.S. Chen, H. Kita, *Ind. Eng. Chem. Res.* 53 (2014) 19168–19174.
- [56] I. Kumakiri, K. Hashimoto, Y. Nakagawa, Y. Inoue, Y. Kanehiro, K. Tanaka, H. Kita, *Catal. Today*. 236 (2014) 86–91.
- [57] C. Ortega, R. Lopez, J. Cacho, V. Ferreira, *J. Chromatogr. A* 923 (2001) 205–214.
- [58] R. Sander, *Atmos. Chem. Phys.* 15 (2015) 4399–4981.
- [59] J.J. Rodríguez-Bencomo, C. Muñoz-González, I. Andújar-Ortiz, P.J. Martín-Álvarez, M.V. Moreno-Arribas, M.Á. Pozo-Bayón, *J. Sci. Food Agric.* 91 (2011) 2484–2494.
- [60] A. Gambuti, A. Rinaldi, M.T. Lisanti, R. Pessina, L. Moio, *Eur. Food Res. Technol.* 233 (2011) 647–655.
- [61] P. Peng, Y. Lan, L. Liang, K. Jia, *Biotechnol. Biofuels* 14 (2021), 10.
- [62] M.H. Zhu, Z.J. Feng, X.M. Hua, H. long Hu, S.L. Xia, N. Hu, Z. Yang, I. Kumakiri, X. S. Chen, H. Kita, *Microporous Mesoporous Mater.* 233 (2016) 171–176.
- [63] K.I. Okamoto, H. Kita, K. Horii, K. Tanaka, M. Kondo, *Ind. Eng. Chem. Res.* 40 (2000) 163–175.
- [64] R.W. Baker, J.G. Wijmans, Y. Huang, *J. Memb. Sci.* 348 (2010) 346–352.
- [65] C. Abels, F. Carstensen, M. Wessling, *J. Memb. Sci.* 444 (2013) 285–317.
- [66] R.D. Offeman, C.N. Ludvik, *J. Memb. Sci.* 367 (2011) 288–295.
- [67] Ó. de la Iglesia, R. Mallada, M. Menéndez, J. Coronas, *Chem. Eng. J.* 131 (2007) 35–39.